J Electr Eng Technol.2018; 13(4): 1558-1565
http://doi.org/10.5370/JEET.2018.13.4.1558

ISSN(Print) 1975-0102
ISSN(Online) 2093-7423

Variable-magnitude Voltage Signal Injection for Current Reconstruction in an IPMSM Sensorless Drive with a Single Sensor

Jun-Hyuk Im*, Sang-Il Kim* and Rae-Young Kim†

Abstract – Three-phase current is reconstructed from the dc-link current in an AC machine drive with a single current sensor. Switching pattern modification methods, in which the magnitude of the effective voltage vector is secured over its minimum, are investigated to accurately reconstruct the three-phase current. However, the existing methods that modify the switching pattern cause voltage and current distortions that degrade sensorless performance. This paper proposes a variable-magnitude voltage signal injection method based on a high frequency voltage signal injection. The proposed method generates a voltage reference vector that ensures the minimum magnitude of the effective voltage vector by varying the magnitude of the injection signal. This method can realize high quality current reconstruction without switching pattern modification. The proposed method is verified by experiments in a 600W Interior permanent magnet synchronous machine (IPMSM) drive system.

Keywords: Current reconstruction, High frequency voltage signal injection, IPMSM, Single current sensor.

1. Introduction

An AC machine drive system using a voltage source inverter requires information of three-phase currents and rotor position for instant torque control [1]. A typical drive system uses two or three current sensors to measure three-phase currents, and a position sensor to detect a rotor position; however, there are several problems in systems using sensors, such increased cost and the volume, and reduced reliability due to the possibility of sensor failure. In low-cost drive systems such as home appliances, sensor cost makes up a large portion of the overall product cost.

Researchers have attempted to reduce the number of sensors and therefore the cost of these systems [2, 3]. One approach utilizes a single current sensor at the dc-link stage to reconstruct the phase current [4-7]. Based on the relationships between the dc-link current and the phase current in various switching states of the inverter, two-phase currents can be reconstructed from the dc-link current with the given voltage vector in every PWM period. However, the phase current cannot be reconstructed from the dc-link current when the effective voltage vector is not secured over the minimum magnitude. While switching pattern modification methods for securing the minimum magnitude of the effective voltage vector are widely used to solve this problem [4-6], these methods result in distorted voltage and current, as well as reductions in the linear modulation region.

Another approach to reducing the number of sensor is a sensorless method that removes the position sensor [8-13]. The position sensorless control method can be classified into a machine-model-based method and a signal injection method according to the position estimation principle. The machine-model-based method is based on the back electromotive force (BEMF) and is simple to implement, which shows good control performance in the mid- or high-speed operation region [8-10]. The signal injection method extracts the rotor position information from the magnetic saliency of the machine. Since this physical property tends to be speed-independent, this method can be used in zero- or low-speed operation region [11-13].

Recently, research has been conducted to apply sensorless controls in drive systems with a single current sensor for further cost reduction. Reference [14] proposed a machine-model sensorless control method using a single current sensor and its performance was compared to that of the full-sensor control. Reference [15] proposed a signal injection sensorless control method using a single current sensor. However, these methods are still based on the switching pattern modification, and thus result in degraded sensorless control performance.

In this paper, a variable-magnitude voltage signal injection sensorless method that can secure the minimum magnitude of the effective voltage vector without a switching pattern modification is proposed. Firstly, the existing signal injection sensorless control methods are analyzed in drive systems with a single current sensor. Based on this analysis, we propose a method to change the magnitude of the injection signal in the stationary reference frame. The proposed method generates the voltage reference vector that ensures the minimum magnitude of the effective voltage vector. This method

† Corresponding Author: Dept. of Electrical and Biomedical Engineering, Hanyang University, Korea. (rykim@hanyang.ac.kr)
* Dept. of Electrical Engineering, Hanyang University, Korea. ({opaljh, si401}@hanyang.ac.kr)
Received: September 18, 2017; Accepted: February 5, 2018

Table 1. Relation between the dc-link current and phase current for effective voltage vector

$\vec{V}_n$	$\vec{V}_0$	$\vec{V}_1$	$\vec{V}_2$	$\vec{V}_3$	$\vec{V}_4$	$\vec{V}_5$	$\vec{V}_6$	$\vec{V}_7$
i_{dc}	0	i_a	$-i_c$	i_b	$-i_a$	i_c	$-i_b$	0

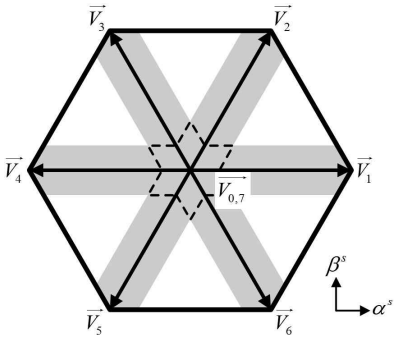

Fig. 1. Immeasurable area (gray) in the stationary reference frame

enables high quality current reconstruction without switching pattern modification, which can minimize voltage and current distortion. The proposed method is verified by experiments in a 600W IPMSM drive system.

2. Current Reconstruction Technique

2.1 Conventional current reconstruction

The relationship between the dc-link current and the phase current for the effective voltage vector is detailed in Table 1, where $\vec{V}_n$ consists of the effective voltage vectors ($\vec{V}_1 - \vec{V}_6$), and the zero voltage vectors ($\vec{V}_0$ and $\vec{V}_7$). Note that when $\vec{V}_0$ and $\vec{V}_7$ are applied, the phase current cannot be reconstructed, since dc-link current i_{dc} does not flow.

The space vector PWM (SVPWM) is widely used for three-phase machine control. Each half switching period has two effective voltage vectors, and therefore, the phase currents of two phases can be reconstructed from i_{dc} using Table 1, and the current of the other phase can be calculated under the assumption of a balanced three-phase system.

To reconstruct the phase current using this technique, a minimum effective voltage vector is required to secure the minimum duration time of the effective voltage vector. The minimum duration time T_{min} can be represented as (1), where T_{dead} denotes the dead time of the three-phase inverter, T_{ADC} is the analog-to-digital conversion time, and T_{sett} is the settling time of i_{dc}.

$$T_{\min} \geq T_{dead} + T_{ADC} + T_{sett} \tag{1}$$

The shaded area shown in Fig. 1 represents an

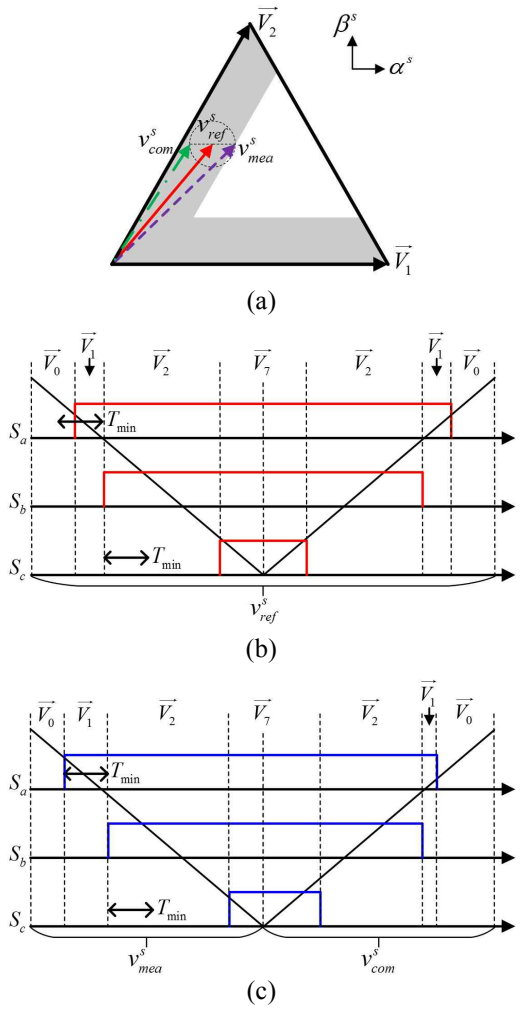

Fig. 2. PWM switching pattern modification. (a) voltage vectors in the stationary reference frame, (b) original PWM switching patterns, and (c) modified PWM switching patterns

immeasurable area in case T_{min} cannot be secured. When the voltage reference vector is located outside the dashed line in the immeasurable area, only one effective voltage vector can secure T_{min}, so that only one phase current can be reconstructed. When the voltage reference vector is located inside the dashed line, the phase current cannot be reconstructed, since both of the two effective voltage vectors are small than the minimum magnitude that can secure T_{min}.

2.2 Current reconstruction based on the PWM switching pattern modification

Several methods have been proposed to successfully reconstruct three-phase currents even in the immeasurable area. The switching pattern modification method, for example, adjusts the magnitude of the effective voltage vector [4-6]. When the voltage reference vector is located in the immeasurable area, the effective voltage vector is

forcibly increased to the minimum magnitude to secure T_{min} necessary for the current reconstruction.

For example, when the final voltage reference vector v^s_{ref} is located in the immeasurable area shown in Fig. 2(a), $\overrightarrow{V_2}$ has a large enough magnitude to accurately reconstruct the C-phase current i_c from i_{dc}, while $\overrightarrow{V_1}$ does not have a sufficiently large magnitude to obtain the A-phase current i_a shown in Fig. 2(b). Therefore, three-phase currents cannot be successfully reconstructed. Fig. 2(c) shows an example applying the switching phase-shift method, which is one of the switching pattern modification methods [16]. This method adjusts the magnitude of the effective voltage vectors to secure T_{min} for current reconstruction. As shown in Fig. 2(a), v^s_{ref} is replaced with the measurement voltage vector v^s_{mea} and the compensation voltage vector v^s_{com}. As shown in Fig. 2(c), it is possible to secure the minimum magnitude of two effective voltage vectors in the immeasurable area, and the averaged voltage reference during a switching period can be maintained, as shown in Fig. 2(a). While three-phase currents can be successfully reconstructed in this fashion, the voltage waveform is distorted due to the switching pattern modification, which causes current distortion, torque ripple, and deterioration of sensorless control performance.

3. High Frequency Voltage Signal Injection Sensorless Control with Single Current Sensor

High frequency voltage signal injection sensorless control methods, including a pulsating voltage signal injection method in the estimated rotor reference frame, and a rotating voltage signal injection method in the stationary reference frame are studied in [11-13]. In this section, the high frequency voltage signal injection sensorless control methods are analyzed in the drive system with a single current sensor. v^s_{ref} is influenced according to the high frequency voltage signal injection methods.

3.1 Pulsating voltage signal injection in the estimated rotor reference frame

Fig. 3 shows the waveform and the trajectory of the voltage reference vector in a pulsating voltage signal injection method in the estimated rotor reference frame.

When a sinusoidal voltage signal of $f_{sw}/8$ frequency is injected, the voltage signal of the waveform as shown in Fig. 3(a) is injected into the *d*-axis of the estimated rotor reference frame. When the rotor position is at 0° as shown in Fig. 3(a), all of the voltage reference vectors exist inside the immeasurable area; whereas, when the rotor position is at 30° as shown in Fig. 3(b), most of the voltage reference vectors exist outside the immeasurable area. Therefore, when the pulsating voltage signal injection method is used, the voltage reference vectors are located in the immeasurable area according to the rotor position, and

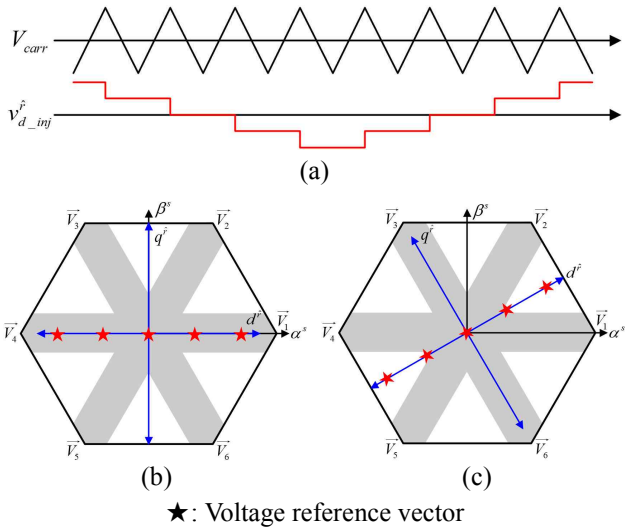

Fig. 3. Waveform and trajectory of voltage reference vectors in pulsating voltage signal injection in the estimated rotor reference frame (a) $f_{sw}/8$ Hz sinusoidal voltage signal (b) at $\theta_r = 0^\circ$, and (c) at $\theta_r = 30^\circ$

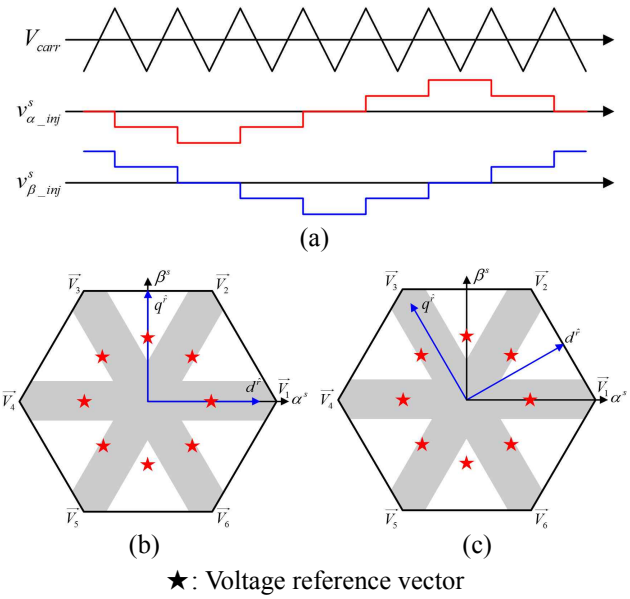

Fig. 4. Waveform and trajectory of voltage reference vectors in rotating voltage signal injection in the stationary reference frame (a) $f_{sw}/8$ Hz sinusoidal voltage signal (b) at $\theta_r = 0^\circ$, and (c) at

the current reconstruction is not possible.

3.2 Rotating voltage signal injection in the stationary reference frame

Fig. 4 shows the waveform and trajectory of the voltage reference vector using the rotating voltage signal injection method in a stationary reference frame. Assuming the same

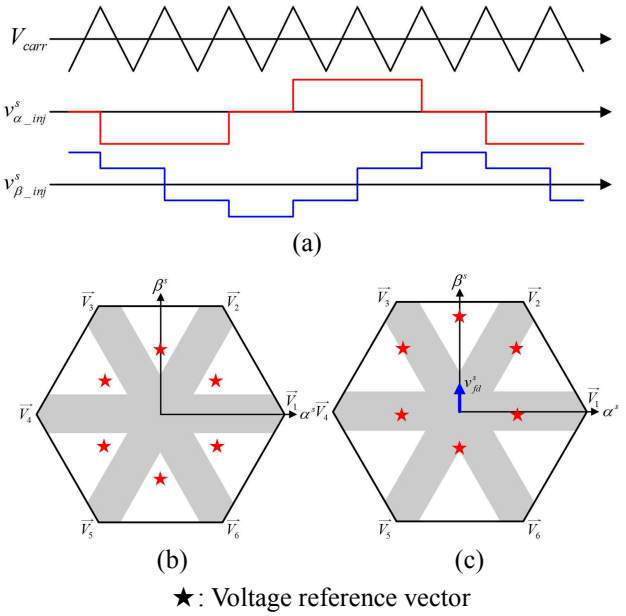

Fig. 5. Waveform and trajectory of voltage reference vectors in rotating voltage signal injection in the stationary reference frame (a) f_{sw}/6 Hz sinusoidal voltage signal under (b) no load condition, and (c) load condition

injection frequency as Fig. 3, the injected voltage signal is as shown in Fig. 4(a). Fig. 4(b) and Fig. 4(c) show the trajectory of the voltage reference vectors when the rotor position is located at 0°and 30°, respectively. Unlike the pulsating voltage signal injection method, the voltage reference vectors are located at constant positions regardless of the rotor position. Some voltage reference vectors still exist in the immeasurable area.

Fig. 5 shows the result of injecting the rotating voltage signal with f_{sw}/6, as shown in Fig. 5(a). Comparing Fig. 4(b) with Fig. 5(b), the positions of the voltage reference vectors are located outside the immeasurable area despite having the same rotor position. However, as shown in Fig. 5(c), in the case of a load condition in which the fundamental voltage reference vector v^s_{fd} exists, v^s_{ref} may be located inside the immeasurable area. Therefore, when the rotating voltage signal injection method is used, the voltage reference vectors are located in the immeasurable area according to the injection frequency and the load condition regardless of the rotor position, and current reconstruction becomes impossible.

4. Proposed Method

Based on the above analysis, we propose a high frequency voltage signal injection sensorless control method suitable for drive systems with a single current sensor. The proposed method is used to vary the magnitude of the injection voltage signal according to the magnitude of v^s_{fd} in the stationary reference frame. Using the proposed

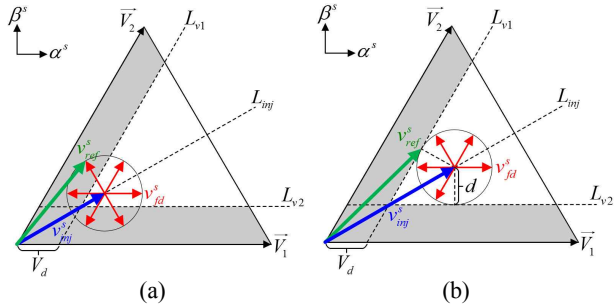

Fig. 6. Voltage reference vectors in Sector 1 of the stationary reference frame according to (a) small injection voltage vector, and (b) large injection voltage vector

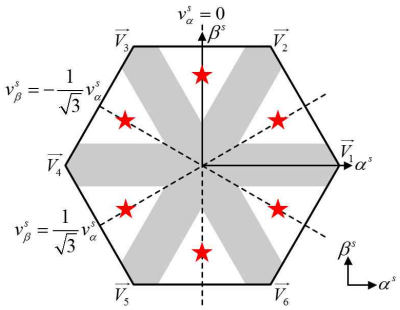

Fig. 7. Linear equations of rotating voltage signal injection in the stationary reference frame

method, a high quality current reconstruction can be realized without switching pattern modification by generating v^s_{ref}, ensuring that the effective voltage vector is larger than the minimum magnitude.

Fig. 6 shows the injection voltage vector of f_{sw}/6 frequency $v^s_{inj}(v^s_{\alpha\_inj}, v^s_{\beta\_inj})$, the fundamental voltage reference vector $v^s_{fd}(v^s_{\alpha\_fd}, v^s_{\beta\_fd})$, and v^s_{ref} in Sector 1 according to the magnitude of the injection voltage vector, where superscript s denotes the stationary reference frame, $v^s_{\ a}$ is the α -axis voltage of the stationary reference frame, and $v^s_{\ \beta}$ is the β -axis voltage of the stationary reference frame, respectively.

As shown in Fig. 6(a), if the magnitude of v^s_{inj} is small with constant, v^s_{ref} may be located in the immeasurable area according to v^s_{fd}. However, as shown in Fig. 6(b), if the magnitude of v^s_{inj} is appropriately adjusted, v^s_{ref} can always exist outside the immeasurable area regardless of v^s_{fd}. Therefore, v^s_{ref}, the sum of v^s_{fd} and v^s_{inj}, has to be determined at the boundary of the circle with the radius d of v^s_{fd} centered on the location of v^s_{inj} to ensure that v^s_{ref} always exists outside the immeasurable area. We must determine v^s_{inj} such that the circle with radius d is in contact with the border of the immeasurable area. To do this, we can utilize the distance formula between a point and a straight line.

The boundaries of the immeasurable area can be expressed as linear equations as shown in Fig. 6. In case of the rotating voltage signal injection method in the

Table 2. Variable-magnitude voltage signal injection

Sector No.	$v^s_{\alpha\_inj}$	$v^s_{\beta\_inj}$
1	$\sqrt{3}d+\frac{3}{2}V_d$	$d+\frac{\sqrt{3}}{2}V_d$
2	0	$2d+\sqrt{3}V_d$
3	$-\left(\sqrt{3}d+\frac{3}{2}V_d\right)$	$d+\frac{\sqrt{3}}{2}V_d$
4	$-\left(\sqrt{3}d+\frac{3}{2}V_d\right)$	$-\left(d+\frac{\sqrt{3}}{2}V_d\right)$
5	0	$-\left(2d+\sqrt{3}V_d\right)$
6	$\sqrt{3}d+\frac{3}{2}V_d$	$-\left(d+\frac{\sqrt{3}}{2}V_d\right)$

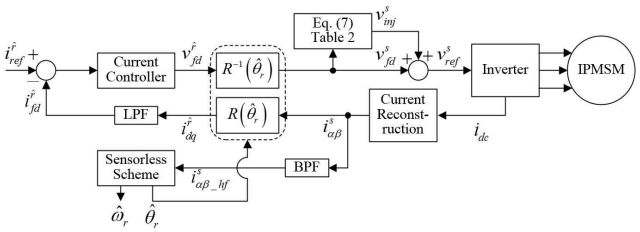

Fig. 8. Block diagram of the high frequency voltage signal injection sensorless control using the proposed method

stationary reference frame, the location of v^s_{inj} is constant, and then its position can also be expressed by linear equations as shown in Fig. 7.

For example, v^s_{inj}, which is a distance d away from the boundary L_{v2} of the immeasurable area in (2), can be derived as (3) using the distance formula between a point and a straight line:

$$L_{v2}: v^s_\beta = \frac{\sqrt{3}}{2}V_d \tag{2}$$

$$d = \frac{\left|0\left(v^s_{\alpha\_inj}\right)+1\left(v^s_{\beta\_inj}\right)-\frac{\sqrt{3}}{2}V_d\right|}{\sqrt{0^2+1^2}}. \tag{3}$$

Since v^s_{inj} has the relation as (4), it can be defined as in (5):

$$L_{inj}: v^s_{\beta\_inj} = \frac{1}{\sqrt{3}}v^s_{\alpha\_inj} \tag{4}$$

$$v^s_{inj}\left(v^s_{\alpha\_inj}, v^s_{\beta\_inj}\right) = \left(v^s_{\alpha\_inj}, \frac{v^s_{\alpha\_inj}}{\sqrt{3}}\right). \tag{5}$$

Therefore, v^s_{inj} can be obtained as (6), where d is defined as (7) and V_d is the minimum magnitude of the effective voltage vector for current reconstruction:

$$v^s_{inj} = \left(\sqrt{3}d+\frac{3}{2}V_d, d+\frac{\sqrt{3}}{2}V_d\right). \tag{6}$$

$$d = \sqrt{{v^s_{\alpha\_fd}}^2 + {v^s_{\beta\_fd}}^2} \tag{7}$$

To generalize, v^s_{inj} for each sector is listed in Table 2. Therefore, when v^s_{inj} listed in Table 2 is sequentially applied from Sector 1 through Sector 6, the final voltage reference vector always exists outside the immeasurable area, regardless of the load condition. As a result, a high quality current reconstruction can be realized without the switching pattern modification.

Fig. 8 shows a block diagram of the high frequency voltage signal injection sensorless control with a single current sensor using the proposed method. It can be seen that the phase current $i^s_{\alpha\beta}$ in the stationary reference frame is reconstructed from i_{dc} of the inverter. As v^s_{inj} is injected by Table 2 and (7) according to the proposed method, it can be confirmed that the conventional PWM switching pattern modification is not used. As a result, voltage and current distortion by the switching pattern modification can minimize, which enables high quality current reconstruction.

5. Experimental Results

The proposed method was verified by experiments in the 600W IPMSM drive system as shown in Fig. 9. Table 3 shows the parameters of the IPMSM drive system. The hall-effect current sensors that have sufficient bandwidth and linearity were used for the dc-link current and three-phase current measurements. The PWM switching frequency fsw was chosen to be 5kHz because this will allow to extract the high frequency current component for the IPMSM with a single current sensor. T_{min} was selected to be 8 μs by considering to be longer than the sum of times T_{dead}, T_{ADC}, and T_{sett}. V_d at the selected T_{min} is

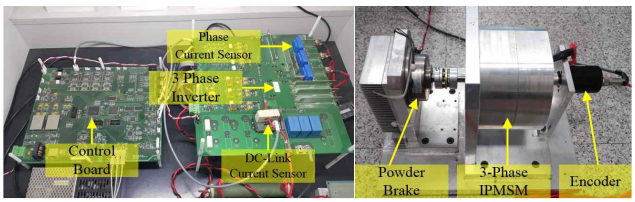

Fig. 9. IPMSM drive system

Table 3. IPMSM drive system parameters

Symbol	Quantity	Value
P_{rate}	Rated power	600 W
T_{rate}	Rated torque	1.6 Nm
P	Poles pairs	3
R_s	Stator resistance	1.65 Ω
L_d	d-axis inductance	11.5 mH
L_q	q-axis inductance	20 mH
λ_{pm}	Rotor magnet flux linkage	0.109 Wb
f_{sw}	PWM switching frequency	5 kHz
V_d	Minimum active voltage vector magnitude	16 V

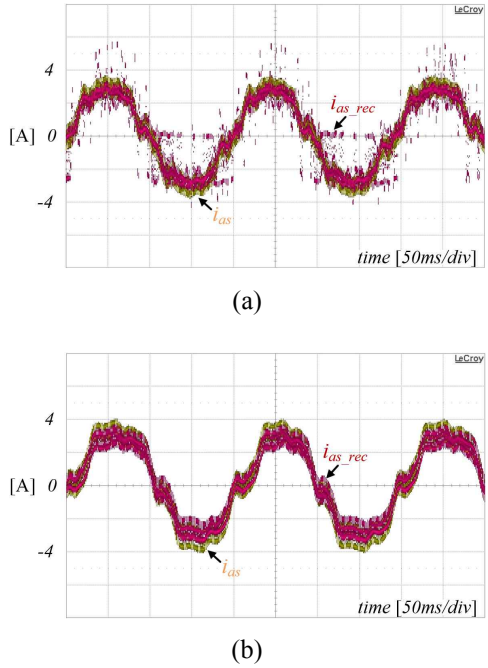

Fig. 10. Reconstructed and measured A-phase currents: (a) without and (b) with the proposed method

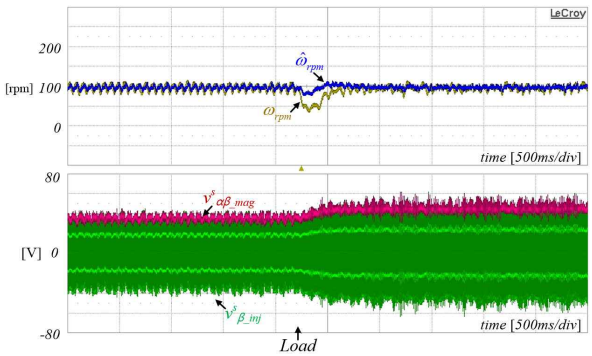

Fig. 11. Sensorless control performance under the step full load using the proposed method

calculated as 16 V.

Fig. 10 shows the reconstructed and measured A-phase currents in the case controlled by phase current measurement with and without the proposed method. As shown in Fig. 10(a), if the magnitude of v^s_{inj} is constant as the conventional rotating voltage signal injection method in the stationary reference frame, v^s_{ref} is located in the immeasurable area according to v^s_{fd}. As a result, the effective voltage vector cannot secure the minimum magnitude and the reconstructed A-phase current i_{as_rec} is distorted. On the other hand, as shown in Fig. 10(b), if the magnitude of v^s_{inj} is varied by the proposed method, v^s_{ref} can always exist outside the immeasurable area regardless of v^s_{fd}. As a result, the effective voltage vector can always secure the minimum magnitude and i_{as_rec} properly reflect the measured A-phase current i_{as}.

Fig. 11 shows the sensorless control performance of

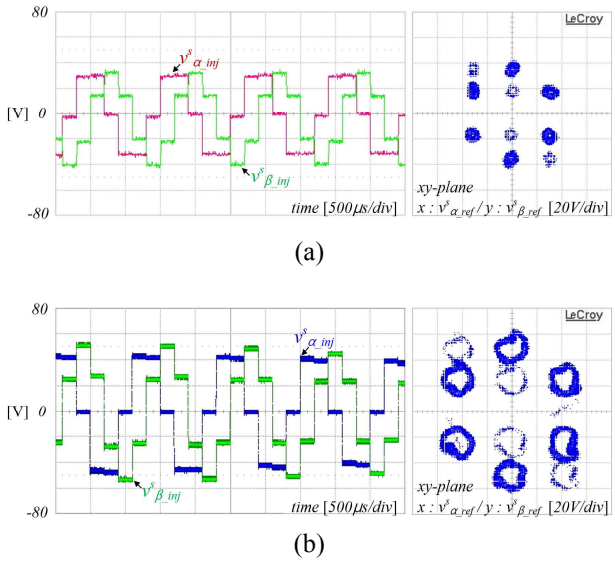

Fig. 12. Waveform and trajectory of voltage reference vectors by the proposed method under (a) no load and (b) full load

the proposed method in the case controlled by dc-link current measurement under step full load at 100 rpm. The magnitude of the injection voltage signal $v^s_{a\beta\_mag}$ is approximately 38 V under no load condition. When the step full load is applied, the proposed method increase $v^s_{a\beta\_mag}$ as the magnitude of the fundamental voltage reference vector increases, and then $v^s_{a\beta\_mag}$ is approximately 48 V under full load condition, where $v^s_{\beta\_inj}$ is the β-aixs injection voltage signal in the stationary reference frame. It can be confirmed that the rotor speed is controlled at 100 rpm and the estimated rotor speed $\hat{\omega}_{rpm}$ is tracked to the real rotor speed ω_{rpm}. When the step full load is applied, ω_{rpm} and $\hat{\omega}_{rpm}$ are different in the transient state because the speed observer does not sufficiently estimate the load torque variation.

Fig. 12 shows the waveform of v^s_{inj} and the trajectory of v^s_{ref} according to each load condition. As shown in Fig. 10(a), since the magnitude of v^s_{ref} is almost zero in the no load steady state, the trajectory of v^s_{ref} is the same as the trajectory of v^s_{inj}. The trajectory of v^s_{ref} exists outside the immeasurable area due to the voltage signal injection at a $f_{sw}/6$ frequency. Fig. 11(b) presents the results in the full load steady state. As shown in Fig. 11(b), the trajectory of v^s_{ref} can be seen to exist outside the immeasurable area by varying the magnitude of v^s_{inj} using the proposed method. Some trajectory that appear to be in immeasurable area of the *xy*-plane is due to sampling the transient state of the DAC.

6. Conclusion

In this paper, a high frequency voltage signal injection sensorless control method suitable for a drive system with

a single current sensor was proposed. In the proposed method, the magnitude of the high frequency injection voltage signal is varied according to the magnitude of the fundamental voltage reference vector based on the distance formula between a point and a straight line. This results in the final voltage reference vector always existing outside the immeasurable area. High quality current reconstruction can therefore be realized without the switching pattern modification and the voltage and current distortion can be reduced. However, it is not suitable for the high speed range because the magnitude of the high frequency injection voltage signal increases according to the rotor speed. The proposed method was validated through the 600W IPMSM drive system with a single current sensor.

Acknowledgements

This work was supported by "Human Resources Program in Energy Technology" of the Korea Institute of Energy Technology Evaluation and Planning (KETEP), granted financial resource from the Ministry of Trade, Industry & Energy, Republic of Korea (No. 20164010200860).

References

[1] R. Moncada, J. Tapia, and T. Jahns, "Analysis of negative-saliency permanent-magnet machines," *IEEE Trans. Ind. Electron.*, vol. 57, no. 1, pp. 122-127, Jan. 2010.

[2] W. C. Lee, T. K. Lee, and D. S. Hyun, "Comparison of single-sensor current control in the DC link for three-phase voltage-source PWM converters," *IEEE Trans. Ind. Electron.*, vol. 48, no. 3, pp. 491-505, Jun. 2001.

[3] S. I. Kim, J. H. Im, E. Y. Song, and R. Y. Kim, "A new rotor position estimation method of IPMSM using all-pass filter on high-frequency rotating voltage signal injection," *IEEE Trans. Ind. Electron.*, vol. 63, no. 10, pp. 6499-6509, Oct. 2016.

[4] H. Kim and T. M. Jahns, "Phase current reconstruction for AC motor drives using a DC link single current sensor and measurement voltage vectors," *IEEE Trans. Power Electron.*, vol. 21, no. 5, pp. 1413-1419, Sep. 2006.

[5] Y.-S. Lai, Y.-K. Lin, and C.-W. Chen, "New hybrid pulsewidth modulation technique to reduce current distortion and extend current reconstruction range for a three-phase inverter using only DC-link sensor," *IEEE Trans. Power Electron.*, vol. 28, no. 3, pp. 1331-1337, Mar. 2013.

[6] H. Lu, X. Cheng, W. Qu, S. Sheng, Y. Li, and Z. Wang, "A three-phase current reconstruction technique using single DC current sensor based on TSPWM," *IEEE Trans. Power Electron.*, vol. 29, no. 3, pp. 1542-1550,Mar. 2014.

[7] B. Saritha and P. A. Janakiraman, "Sinusoidal three-phase current reconstruction and control using a DC-link current sensor and a curve-fitting observer," *IEEE Trans. Ind. Electron.*, vol. 54, no. 5, pp. 2657-2664, Oct. 2007.

[8] S. Morimoto, K. Kawamoto, M. Sanada, and Y. Takeda, "Sensorless control strategy for salient-pole PMSM based on extended EMF in rotating reference frame," *IEEE Trans. Ind. Appl.*, vol. 38, no. 4, pp. 1054-1061, Jul./Aug. 2002.

[9] M. Rashed, P. F. A. MacConnell, A. F. Stronach, and P. Acarnley, "Sensorless indirect-rotor-field-orientation speed control of a permanent-magnet synchronous motor with stator-resistance estimation," *IEEE Trans. Ind. Electron.*, vol. 54, no. 3, pp. 1664-1675, Jun. 2007.

[10] G. Wang, G. Zhang, Z. Gui, and D. Xu, "Position Estimation Error Reduction Using Recursive-Least-Square Adaptive Filter for Model-Based Sensorless Interior Permanent-Magnet Synchronous Motor Drives," *IEEE Trans. Ind. Electron.*, vol. 61, no. 9, pp. 5115-5125, Sep. 2014.

[11] F. Genduso, R. Miceli, C. Rando, and G. R. Galluzzo, "Back EMF sensorless-control algorithm for high-dynamic performance PMSM," *IEEE Trans. Ind. Electron.*, vol. 57, no. 6, pp. 2092-2100, Jun. 2010.

[12] S. C. Yang and Y. L. Hsu, "Full speed region sensorless drive of permanentmagnet machine combining saliency-based and back-emf-based drive," *IEEE Trans. Ind. Electron.*, vol. 64, no. 2, pp. 1092-1101, Feb. 2017.

[13] Y. D. Yoon, S.-K. Sul, S. Morimoto, and K. Ide, "High-bandwidth sensorless algorithm for ac machines based on square-wave-type voltage injection," *IEEE Trans. Ind. Appl.*, vol. 47, no. 3, pp. 1361-1370, May/ Jun. 2011.

[14] M. Carpaneto, P. Fazio, M. Marchesoni, and G. Parodi, "Dynamic performance evaluation of sensorless permanent-magnet synchronous motor drives with reduced current sensors," *IEEE Trans. Ind. Electron.*, vol. 59, no. 12, pp. 4579-4589, Dec. 2012.

[15] S. C. Yang, "Saliency-Based Position Estimation of Permanent-Magnet Synchronous Machines Using Square-Wave Voltage Injection with a Single Current Sensor," *IEEE Trans. Ind. Appl.*, vol. 51, no. 2, pp. 1561-1571, Mar./Apr. 2015.

[16] Y. Gu, F. Ni, D. Yang and H. Liu, "Switching-state phase shift method for three-phase-current reconstruction with a single DC-link current sensor," *IEEE Trans. Ind. Electron.*, vol. 58, no. 11, pp. 5186-5194. Nov. 2011.

Jun-Hyuk Im He received the B.S. degrees in electronic engineering from Ajou University, Suwon, Korea in 2013. As Unified Master's and Doctor's Course, he has been working in Hanyang University, Seoul, Korea from 2013. His current research interests are power electronics control of electric machines, sensorless motor drives, single current sensor control, electric/hybrid vehicle, and power conversion.

Sang-Il Kim He received the B.S., the M.S., and the Ph.D. degrees in electrical engineering from Hanyang University, Korea, in 1998, 2000, and 2017 respectively. From 2000 to 2005, he was a Researcher with POSCON Company, Korea. From 2005 to 2008, he was a member of the research staff at Samsung Advanced Institute of Technology, Yongin, Korea. Since 2008, he has been a Chief Research Engineer at Doosan Company, Seoul, Korea. His current research interests are power electronics control of electric machines, sensorless drives, electric/hybrid vehicle, and power conversion circuits.

Rae-Young Kim He received the B.S. and M.S. degrees from Hanyang University, Seoul, Korea, in 1997 and 1999, respectively, and the Ph.D. degree from Virginia Polytechnic Institute and State University, Blacksburg, VA, USA, in 2009, all in electrical engineering. From 1999 to 2004, he was a Senior Researcher at the Hyosung Heavy Industry R&D Center, Seoul, Korea. In 2009, he was a Postdoctoral Researcher at National Semiconductor Corporation, Santa Clara, CA, USA, involved in a smart home energy management system. In 2016, he was a Visiting Scholar with the Center for Power Electronics Systems (CPES), Virginia Polytechnic Institute and State University, Blacksburg. Since 2010, he has been with Hanyang University, where he is currently an Assistant Professor in the Department of Electrical and Biomedical Engineering. His research interests include modeling and control of distirbuted power converter systems, soft-switching techniques, energy management systems in microgrid applications, modular power converter for dlswmdrenewable energies and motor drive systems. Dr. Kim was a recipient of the 2007 First Prize Paper Award from the IEEE IAS.